International Journal of Bioprinting

RESEARCH ARTICLE

A new 3D-printed polylactic acid-bioglass composite for bone tissue engineering induces angiogenesis *in vitro* and *in ovo*

Simon Cichos[1], Eva Schätzlein[2], Nadine Wiesmann-Imilowski[3,4], Andreas Blaeser[2,5], Dirk Henrich[6], Johannes Frank[6], Philipp Drees[1], Erol Gercek[1], Ulrike Ritz[1]*

[1]Department of Orthopedics and Traumatology, University Medical Center Mainz, Mainz, Germany

[2]Technical University of Darmstadt, Institute for BioMedical Printing Technology, Darmstadt, Germany

[3]Department of Otorhinolaryngology, University Medical Center Mainz, Mainz, Germany

[4]Department of Oral and Maxillofacial Surgery, University Medical Center Mainz, Mainz, Germany

[5]Technical University of Darmstadt, Centre for Synthetic Biology, Darmstadt, Germany

[6]Department of Trauma, Hand and Reconstructive Surgery, Goethe University Frankfurt, Frankfurt am Main, Germany

(This article belongs to the *Special Issue: Advances in the Application of Bioprinted Biomaterials in Tissue Engineering*)

Abstract

Large bone defects such as those that occur after trauma or resections due to cancer still are a challenge for surgeons. Main challenge in this area is to find a suitable alternative to the gold-standard therapy, which is highly risky, and a promising option is to use biomaterials manufactured by 3D printing. In former studies, we demonstrated that the combination of polylactic acid (PLA) and bioglass (BG) resulted in a stable 3D-printable material, and porous and finely structured scaffolds were printed. These scaffolds exhibited osteogenic and anti-inflammatory properties. This 3D-printed material fulfills most of the requirements described in the diamond concept of bone healing. However, the question remains as to whether it also meets the requirements concerning angiogenesis. Therefore, the aim of this study was to analyze the effects of the 3D-printed PLA-BG composite material on angiogenesis. *In vitro* analyses with human umbilical vein endothelial cells (HUVECs) showed a positive effect of increasing BG content on viability and gene expression of endothelial markers. This positive effect was confirmed by an enhanced vascular formation analyzed by Matrigel assay and chicken chorioallantoic membrane (CAM) assay. In this work, we demonstrated the angiogenic efficiency of a 3D-printed PLA–BG composite material. Recalling the osteogenic potential of this material demonstrated in former work, we manufactured a mechanically stable, 3D-printable, osteogenic and angiogenic material, which could be used for bone tissue engineering.

Keywords: 3D printing; Polylactic acid; Bioglass; Angiogenesis; Vascular formation; *In ovo* CAM assay

***Corresponding author:**
Ulrike Ritz (ritz@uni-mainz.de)

Citation: Cichos S, Schätzlein E, Wiesmann-Imilowski N, *et al*., 2023, A new 3D-printed polylactic acid-bioglass composite for bone tissue engineering induces angiogenesis *in vitro* and *in ovo*. *Int J Bioprint,* 9(5): 751.
https://doi.org/10.18063/ijb.751

Received: February 03, 2023
Accepted: March 04, 2023
Published Online: May 11, 2023

1. Introduction

Large bone defects that occur after trauma or resections due to cancer still are a challenge for surgeons. Often these defects do not heal without supportive therapy, and consequently, the risk to develop nonunions is immense. Autologous bone grafting is the gold standard of therapy for this condition; however, this therapy not only necessitates subsequent surgeries for the patient, but is also associated with side effects and high costs. Moreover, the amount of material is limited[1]. Although some other therapies like reamer-arrigator-aspirator (RIA) systems are getting more and more important[2], main challenge in this area is to find a suitable alternative to the gold-standard therapy, which is highly risky.

One option is to use biomaterials manufactured by 3D printing. Many 3D-printable biopolymers like polylactic acid (PLA), polycaprolacton (PCP), poly lactide-co-glycolide (PGLA), or others are suitable for applications in bone tissue engineering as they are biocompatible, biodegradable, and mechanically stable, but they are not bioactive[3]. One possibility is to combine these materials, for example, polylactide, with bioactive materials like hydroxyapatite (HA)[4], tricalcium phosphate (TCP)[5], or bioglass (BG)[6], resulting in composite demonstrating high osteoconductivity and osteoinductive properties, which are however not printable by themselves. Especially, bioglass is an interesting ionic compound in this context. Bioactive glasses were discovered in 1969 and represent an interesting alternative implant material. 45S5 bioglass (BG) has already been used clinically as it stimulates osteogenesis and forms a strong bond with host tissues[7].

BG has been combined with many different materials, for example, various hydrogels[8], graphene oxide[9], or polycaprolactone[10], from which it is released and induces osteogenic properties[11]. By combining PLA and bioglass, it might be possible to combine the positive characteristics of these materials and overcome their negative aspects.

Back in early 2000s, it was reported that the combination of BG and PLA demonstrated positive effects on bone regeneration[12-14]. The combination of both materials to form a printable composite is a new research area and was reported firstly by Roether *et al.*[14] and Alksne *et al.*[6], who observed high cytocompatibility and osteoinductive properties of the printed PLA–BG scaffolds. Another advantage of the combined material is the degradation process. PLA has been shown to degrade into acid products that might limit tissue regeneration. However, the alkaline nature of BG reduces the acidic side effects of these degradation products[15].

We have recently manufactured a printable material consisting of PLA and increasing concentrations of S53P4 BG up to 20% (w/w). This material was suitable to print complex, porous, and finely structured scaffolds using standard Cartesian 3D printers. In the first step, the porous structure of the material was described, and the mechanical stability was proven[16], showing the potential of this new material. We demonstrated an even distribution of the BG particles within the PLA matrix and a prolonged release of calcium from this material, which increased with BG concentrations. Adhesion of mesenchymal stem cells (MSC) and their osteogenic as well as anti-inflammatory properties increased with increasing BG content of the composite. Accordingly, whole blood stimulation assays followed by protein array analysis revealed no significant inflammatory potential[17,18]. A BG concentration-dependent calcium release from this material[17,16] mediates at least some of the observed effects[18].

Thus, this 3D-printed material fulfills most of the requirements as described in the diamond concept of bone healing—being osteoinductive, osteogenetic, and mechanically stable[19]. However, the question remains as to whether it also meets the requirements concerning angiogenesis[20]. Bone fracture healing is a multifactorial process, with angiogenesis being a key aspect. Without vascularization of the implanted biomaterial, neither bone healing nor any tissue regeneration can take place[21,22]. Known factors involved in formation of vasculature are, for example, stromal derived factor-1 (SDF-1) and vascular endothelial growth factor (VEGF), which also regulate the neoangiogenesis of newly formed bone[22,23]. Further factors or materials that induce angiogenesis are promising to be used in dual-delivery systems to induce angiogenesis in combination with osteogenesis. Further factors or materials are promising to be used in dual-delivery systems to induce angiogenesis in combination with osteogenesis. For example, PLGA was combined with various molecules, for example, VEGF[24,25].

One example besides PLA is the combination of PGLA with various bioactive molecules, for example, VEGF[24,25].

It has been demonstrated in various studies that BG, as one part of composite materials, has positive effects on wound healing[26] and angiogenesis. In combination with collagen, BG induced vascularization of adipose tissue-derived stem cells[27]. Moreover, Deb *et al.*[28] reported co-culture of human osteoblasts and endothelial cells on ceramic-BG scaffolds. Stähli *et al.* and Eldesoqi *et al.* observed a positive effect of BG released from composite materials on endothelial cell morphogenesis[29,30]. A positive effect has also been described for osteochondral regeneration[31].

Therefore, the aim of this study was to analyze the effects of the 3D-printed PLA–BG composite material on

angiogenesis. First, *in vitro* analyses with human umbilical vein endothelial cells (HUVECs) were performed to characterize viability and gene expression of endothelial markers. Differentiation capacity of HUVECs in response to the BG fraction in the test specimen was evaluated by means of reverse transcription polymerase chain reaction (RT-PCR). The effect of the biomaterials on vascular formation was analyzed by Matrigel assay and chicken chorioallantoic membrane (CAM) assay. The goal of this study was to detect whether the 3D-printed PLA–BG composite scaffolds are able to induce angiogenesis in addition to the already detected enhancement of osteogenesis.

2. Methods

2.1. Filament fabrication

Composite filaments of PLA and BG were fabricated as described before[17]. Shortly, PLA granules (PLA-filament Kristall Natur, 3dk.berlin, Berlin, Germany) with a grain size of 2–5 mm and bioglass Type S53P4 (bioglass composition: 53% SiO_2, 23% Na_2O, 20% CaO, 4% P_2O_5, BonAlive Biomaterials Ltd., Turku, Finland) with a grain size of 25–42 µm were mixed manually to obtain compositions with BG content of 0, 5, 10, and 20% (w/w). For filament extrusion, a desktop filament extruder (NEXT 1.0 Advanced, 3devo B.B., Utrecht, the Netherlands) was used. Screw speed was set to 4 U/min and fan speed to 65%. The speed of the conveying mechanism was set to automatic to achieve the desired filament diameter of 1.75 mm.

2.2. Sample fabrication

Two-dimensional round scaffolds of each PLA–BG composite were printed using fused filament fabrication on a 3D printer (i3 MK3S, Prusa Research, Prague, Czech Republic) with a nozzle diameter of 0.4 mm. Filaments were dried at 40°C for at least 12 h. Sample geometries were designed with computer-aided design software NX 12 (Siemens NX 12, Siemens AG, Berlin and Munich, Germany) and preprocessed with Cura Ultimaker v.4.6. (Ultimaker, Utrecht, the Netherlands). A flat disk consisting of two layers with a diameter of 0.5 cm was printed and used for further experiments.

2.3. Biocompatibility assessment

In vitro cytotoxicity was analyzed analogous to ISO 10993-5 using the MTT ([3-(4,5-dimethylthiazol-2-yl)-2,5-diphenyltetrazoliumbromid)]) assay. Mouse L929 cells (20,000 cells/well) were seeded in a 96-well tissue culture plate for 24 h. PLA–BG disks were incubated in 120 µL cell media for 48 h. About 100 µL of this extract were given to L929 cells in the 96-well plate. After an incubation time of 24 h, the MTT assay was performed and the colorimetric readout was performed at a wavelength of 570 nm (reference wavelength 650 nm). Zinc diethyl dithiocarbamate (ZDEC) and zinc dibutyl dithiocarbamate (ZDBC) (Food and Drug Safety Center, Hatano Research Institute, Hadano, Japan) were used as positive controls as they induce a reproducible cytotoxic reaction.

2.4. Cell culture and microscopy

HUVECs were purchased from Promocell (Heidelberg, Germany) and cultured in complete EBM-2 medium (Promocell, Heidelberg, Germany) as recommended by the supplier. For microscopic observations after seeding on PLA-BG samples, cells were labeled with Cell Tracker™ Green according to the manufacturer's instructions (Life Technologies, Carlsbad, CA, USA]. $2 \times 10^5/0.2$ cm^2 HUVECs were seeded onto the different PLA–BG disk and cultivated overnight. The next day cell detection was performed with the EVOS® Digital Inverted Microscope (Life Technologies, Carlsbad, CA, USA).

2.5. Viability

Cell viability was tested with the alamarBlue® assay. $2 \times 10^5/0.2$ cm^2 HUVECs were seeded onto the different PLA–BG disk and cultivated overnight. The alamarBlue® assay (Gibco®Invitrogen™ Life Technologies, Carlsbad, CA, USA) was performed 1 and 4 days after seeding. For this purpose, cells were incubated with 320 µL of a 10% alamarBlue solution in medium for 4 h at 37°C. Subsequently, 100 µL of the supernatant was transferred to a 96-well plate, and the absorbance (presented as fluorescence intensity) of each was measured at 560/600 nm.

2.6. PCR

5×10^4 /0.2 cm^2 HUVECs were seeded onto PLA–BG disks and detached with accutase the next day. The cell suspensions were centrifuged at 1,400 rpm for 5 min and the cell pellet was stored at −80°C for future use. Isolation of RNA was performed using PeqGold Total RNA Micro Kit (PeqLab) according to manufacturer's instruction. Total RNA (1 µg) was reverse-transcribed into cDNA using dNTPs (4you4 dNTPs Mix (10 mM), BIORON GmbH, Ludwigshafen), Random Primers (Promega, Madison, WI, USA), and MuLV RT (M-MuLV Reverse Transcriptase, M0253S New England Biolabs, Ipswich, MA, USA) according to the manufacturer's instructions. For gene expression analyses, cDNA template underwent PCR amplification (40 cycles) using the SYBR Green (PowerUp™ SYBR® Green master mix, Applied Biosystems, Foster City, CA, USA) and sequence-specific primers (primer sequences listed in Table 1). *GAPDH* was used for normalization, and results were calculated using the well-established $2^{-\Delta\Delta Ct}$ method[32].

2.7. Matrigel assay

In this experiment, a series of conditioned media containing pure PLA and BG in different concentrations were prepared

Table 1. Primer sequences

Gene	Forward primer (5′ to 3′)	Reverse primer (5′ to 3′)
GAPDH	CGA CCA CTT TGT CAA GCT CA	AGG GGA GAT TCA TGT TGG TG
CD31	CAT TGG CGT GTT GGG AAG AA	GCT CAT GTT TGC CTA GCT CC
KDR	TTA CTT GCA GGG GAC AGA GG	TTC CCG GTA GAA GCA CTT GT

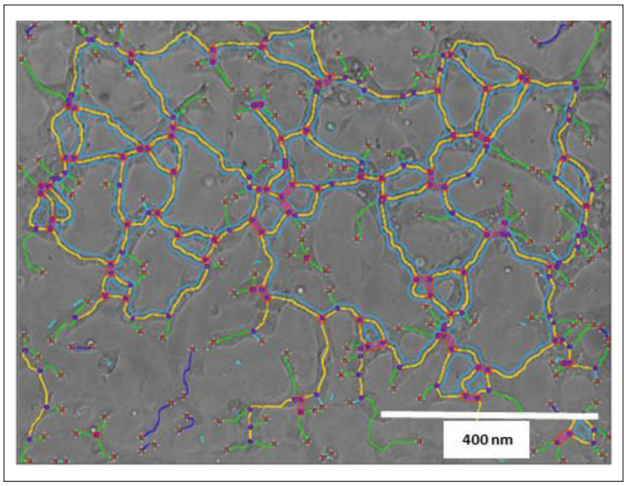

Figure 1. Example of Matrigel analysis[33]. Yellow lanes show the segments, while pink circles represent junctions.

by incubating the media for 48 h so that all solutes can be fully absorbed. 5 × 10^4/100 µL HUVECs were mixed with Matrigel® solution in a 1:1 ratio and then incubated for 30 min to allow the Matrigel® to take its solid form. Afterward, 200 µL of the additive medium was pipetted into each well and incubated for 24 h. The following day, photos were taken under the microscope (EVOS®) and analyzed using ImageJ® (Angiogenesis Analyzer; Figure 1[33]).

2.8. CAM assay

Previous studies have already proven that the CAM assay is well suited for assessing the biocompatibility of biomaterials as well as their angiogenic potential[34,35]. Hens' eggs (Leghorn) were stored horizontally in an incubator (Brutmaschinen Janeschitz GmbH, Hammelburg, Germany) at 37.5°C for 3 days. On day 3 of egg development (EDD 3), 5–6 mL of albumin was removed with a sterile 10-mL syringe and a 21-G × 1-1/2″ needle (0.8 × 40 mm) (BD MicrolanceTM Becton Dickinson GmbH, Heidelberg, Germany) from the blunt end. After albumin removal, the eggshell was opened at the top with autoclaved scissors and subsequently covered with ParafilmVR (Sigma-Aldrich, St. Louis, MO, USA) to prevent evaporation. On day 8 of egg development (EDD 8), PLA–BG disks were placed onto the CAM. Six days after placement fluorescence microscopy was performed, the eggs were placed horizontally under a microscope (Olympus BXFM, OLYMPUS DEUTSCHLAND GmbH, Hamburg, Germany). The analysis of the vascular density was carried out using ImageJ[33].

2.9. Statistical analysis

Statistical analyses were performed using the software GraphPad Prism. The results are presented as medians and quartiles. Measurements were carried out in triplicates. Cell-based experiments were independently repeated three times. Normally distributed data were analyzed by one-way analysis of variance (ANOVA). Depending on Levene's test for equality of variances, pairwise comparisons were conducted either by a Tukey–HSD or Games–Howell *post hoc* test. In contrast, non-normally distributed data were evaluated with the Kruskal–Wallis test followed by a Bonferroni-corrected Conover–Iman analysis. For pairwise comparisons, the Mann–Whitney *U* test was used. $P < 0.05$ was considered statistically significant ($^*P < 0.05$, $^{**}P < 0.01$, $^{***}P < 0.005$, and $^{****}P < 0.001$). Due to multiple testing, the *P*-values were adjusted through Bonferroni–Holm method.

3. Results and discussion

3.1. Sample fabrication

Scanning electron microscopy (SEM) images of the filament were taken, which demonstrate an even distribution of BG particles. For *in vitro* and *in ovo* analyses, simple cylindrical structures containing two layers, with a diameter of 5 mm and a height of 300 µm were printed (Figure 2 and ref. [17]).

3.2. Biocompatibility

In order to ensure biocompatibility of the different PLA–BG scaffolds, the scaffolds were incubated in medium for 48 h, and the resulting supernatants were transferred to L929 cells seeded in 96-well plate for 24 h. After 24 h, in accordance to ISO-10993-5 ("Biological evaluation of medical devices"), a MTT assay was performed. Figure 3 shows the cell viability in different PLA–BG scaffolds compared to controls; the cytotoxic controls show no viability.

3.3. Adhesion

To detect whether BG supports the adhesion capacity of endothelial cells on PLA disks, cells labeled with CellTracker™ Green were seeded on PLA scaffolds with BG in different concentrations. With increasing BG

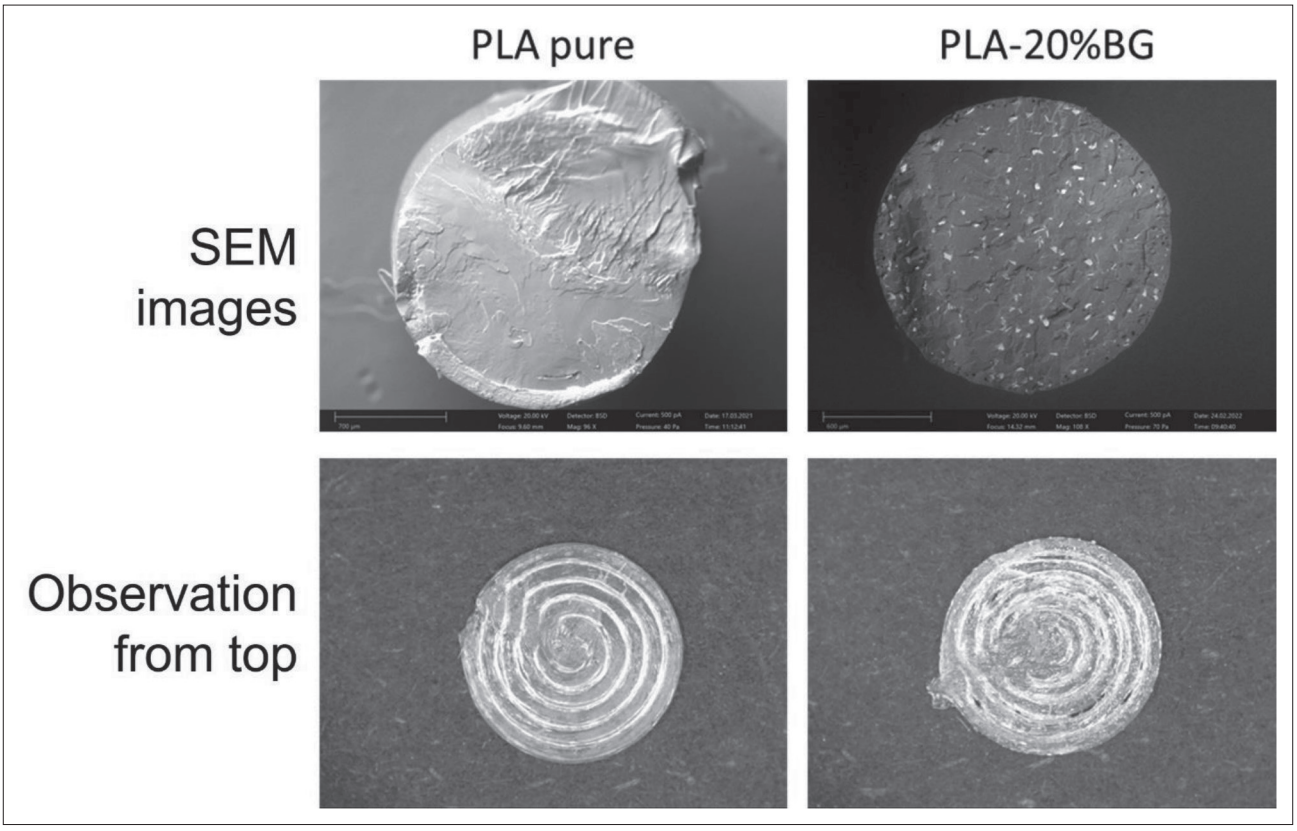

Figure 2. SEM images and gross observation of the 3D-printed PLA pure and PLA–20%BG composite scaffolds.

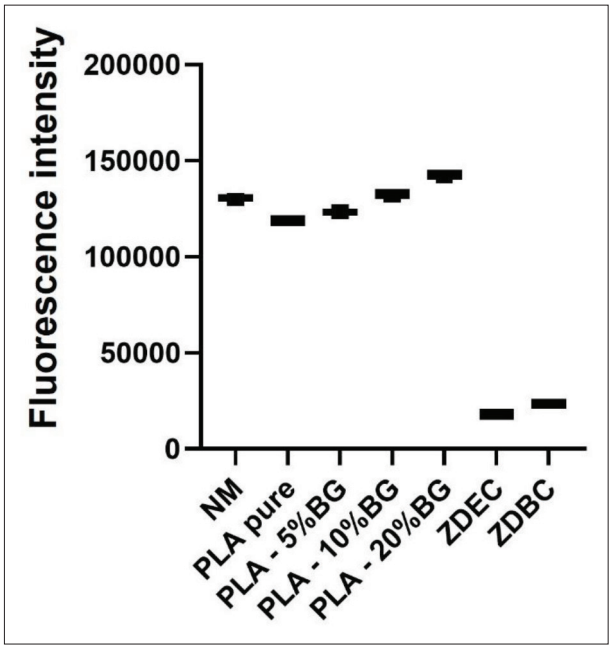

Figure 3. MTT tests performed analogous to ISO 10993-5 confirmed the biocompatibility of all four PLA scaffolds without and with BG in different concentrations. Significant differences were only observed when compared to the cytotoxic controls. NM: normal cultivation medium; ZDEC and ZDBC: cytotoxic controls.

content, an increase in the number of adhered cells could be observed (Figure 4).

3.4. Viability

The positive effect of BG inclusion to PLA was confirmed by viability assays (alamarBlue assay) 1 and 4 days after seeding. On both days, viability of HUVECs on scaffolds with 10% and 20% BG was significantly increased compared to PLA pure and also to PLA-5%BG (day 4; Figure 5). Viability increased significantly on PLA–20%BG from day 1 to day 4, which manifested the best effect in terms of cell viability with respect to other scaffolds with different BG concentrations.

Few studies have analyzed the effect of BG on the viability and proliferation of HUVECs. Li *et al.*[26] tested BG ion extracts in different dilutions on HUVECs proliferation and showed that higher BG concentrations suppressed proliferation of HUVECs. However, their application method is hardly comparable to our experiments as their intention was to induce wound healing. Another study used BG–PVA (polyvinyl alcohol) scaffolds in the ratios of 4:1 and 3:1 and demonstrated an increased proliferation of a HUVEC-hOB coculture in comparison to HA scaffolds[28]. Some studies incorporated BG in different hydrogels and reported positive effects on endothelial cell

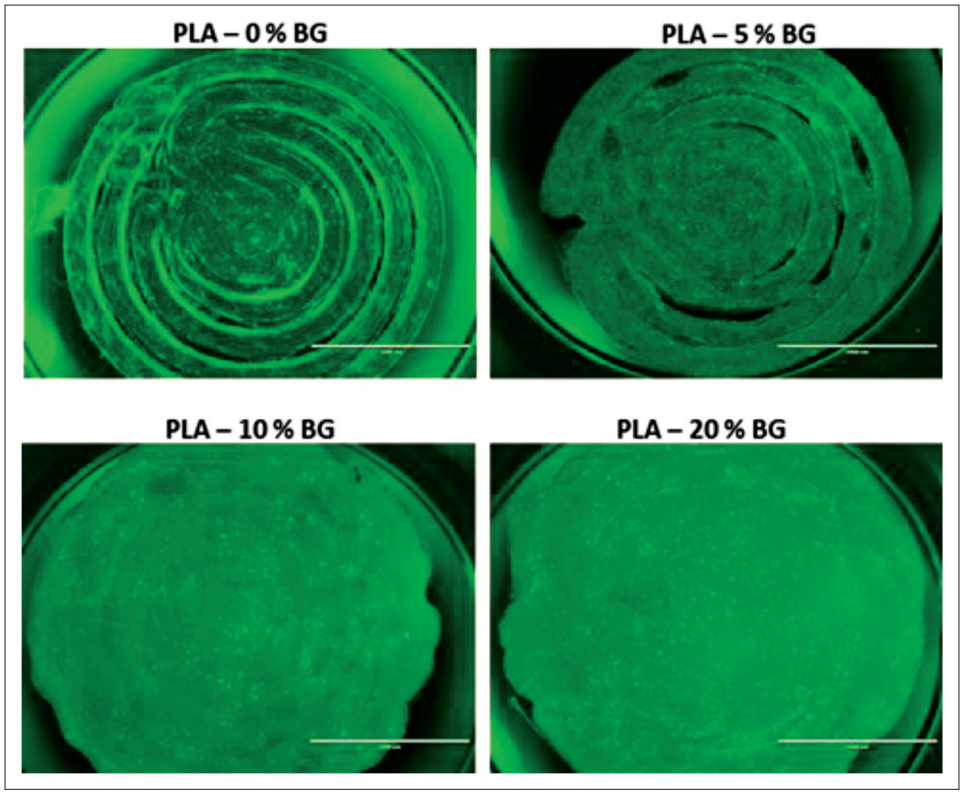

Figure 4. Adhesion of HUVECs (green) to PLA–BG disks. Scale bar: 2 mm.

adhesion and growth as well as on vascularization and wound healing[36,37]. The basic concepts of these studies are comparable to our experimental approach and confirm the positive effect of BG on angiogenesis.

3.5. Gene expression

To confirm the results of the adhesion and viability assays, gene expression analyses of the two endothelial markers *CD31* and *KDR* (kinase insert domain receptor) were performed. Considering the results from this study as well as from the studies regarding osteogenesis, one can conclude that the lowest concentration of BG has no effect on osteogenic or endothelial cells. The group with the lowest BG concentration of 5% was excluded from further studies. Only PLA with BG concentrations from 10% and 20% were used for the following experiments.

Gene expression of both endothelial markers was enhanced in both PLA–10%BG and PLA–20%BG groups when compared to pure PLA-scaffolds. PLA–20%BG showed the highest expression of these endothelial markers (Figure 6). *KDR* expression seems to be lower on day 4 on PLA–20%BG compared to PLA–10%BG; however, the difference is not statistically significant, whereas the difference to PLA pure group is statistically significant.

As already stated before, only few studies have analyzed the effect of BG on vascular gene expression. It has been shown that human dental stromal cells demonstrated a higher gene expression of *CD34*, *CD31*, and *KDR* in 3D BG constructs[38]. This research group also detected osteogenic effects in the same scaffold[39]. Li *et al.*[26] observed a positive effect on gene expression of *FGF* (fibroblast growth factor), *VEGF* and *KDR* in HUVECs after being seeded on BG–PVA scaffolds.

3.6. Angiogenesis assay (Matrigel assay)

To analyze the differentiation capacity of PLA-BG scaffolds, Matrigel assays were performed to quantify tube formation[33,40]. This assay is easy to perform, easy to analyze and quantify, and highly reproducible. Another advantage is that endothelial cells attach within 1 h and start to form tubes as well as cell–cell contacts within 12–24 h[41].

Exemplary illustrations of HUVECs seeded in Matrigel® and incubated with conditioned medium from the three PLA–BG scaffolds (0%, 10%, and 20% BG) are shown in Figure 7A. Figure 7B demonstrates the quantitative analysis showing that all three analyzed components (number of junctions, number of segments, and total length) increased with BG content in the 3D-printed scaffolds (Figure 7).

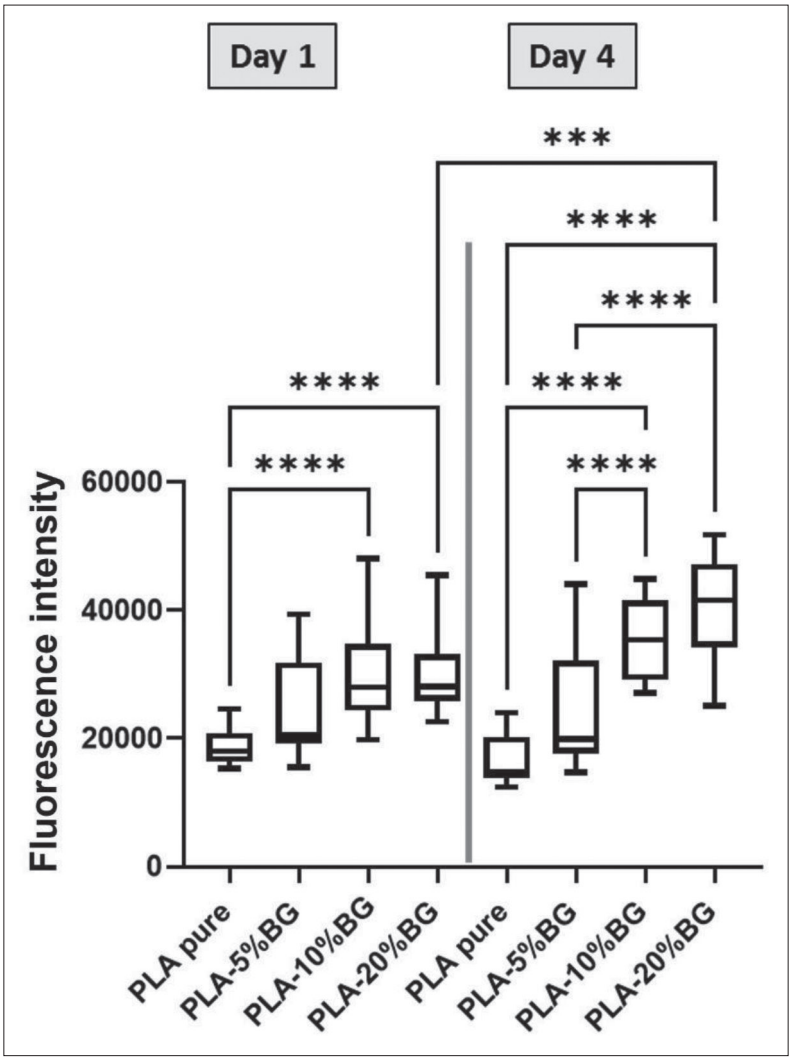

Figure 5. Viability of HUVECs seeded on PLA–BG disks measured with the alamarBlue assay. Viability (presented as fluorescence intensity) increased with BG concentration in the test specimen on day 1 and day 4 in comparison to control. Results are expressed as median and quartiles (n = 9). Mann–Whitney U tests revealed significant differences (*P < 0.05, **P < 0.01, ***P < 0.005; ****P < 0.001). For a better overview, only the significant differences are indicated.

Until now, there are no quantitative data concerning the effects of BG on angiogenesis tested with Matrigel assay. To sum up the *in vitro* results, we can clearly state that the 3D-printed PLA disks with a BG content of 10% or 20% induce angiogenic properties.

3.7. CAM assay

To analyze the neo-vessel formation around the scaffolds as well as its integration into the vascular network, a CAM assay was performed. The CAM assay is a simple, fast, and low-cost model to test angiogenesis *in vivo*[42]. It is an attractive alternative to small animal models and respects the guidelines for a reduction of animal numbers and experiments[43]. Moreover, compared to small animal models, where periods of up to 6 weeks are necessary, the neoangiogenesis on the CAM can be analyzed after 3–7 days[44,45].

Determination of the vascular density around the scaffold showed a significantly higher density 7 days after placement of the PLA–20%BG disks compared to the pure PLA and the PLA–10%BG discs (Figure 8). As negative control, the PLA pure was used. A control without scaffold has not been used as the material itself influences the CAM by friction and weight. Neoangiogenesis around the scaffold was measured to show the effect of the scaffold on vascularization.

Determination of the vascular density around the scaffold demonstrated a significantly higher density 7 days after placement of the PLA–20%BG disks compared to the pure PLA and the PLA–10%BG disks (Figure 8).

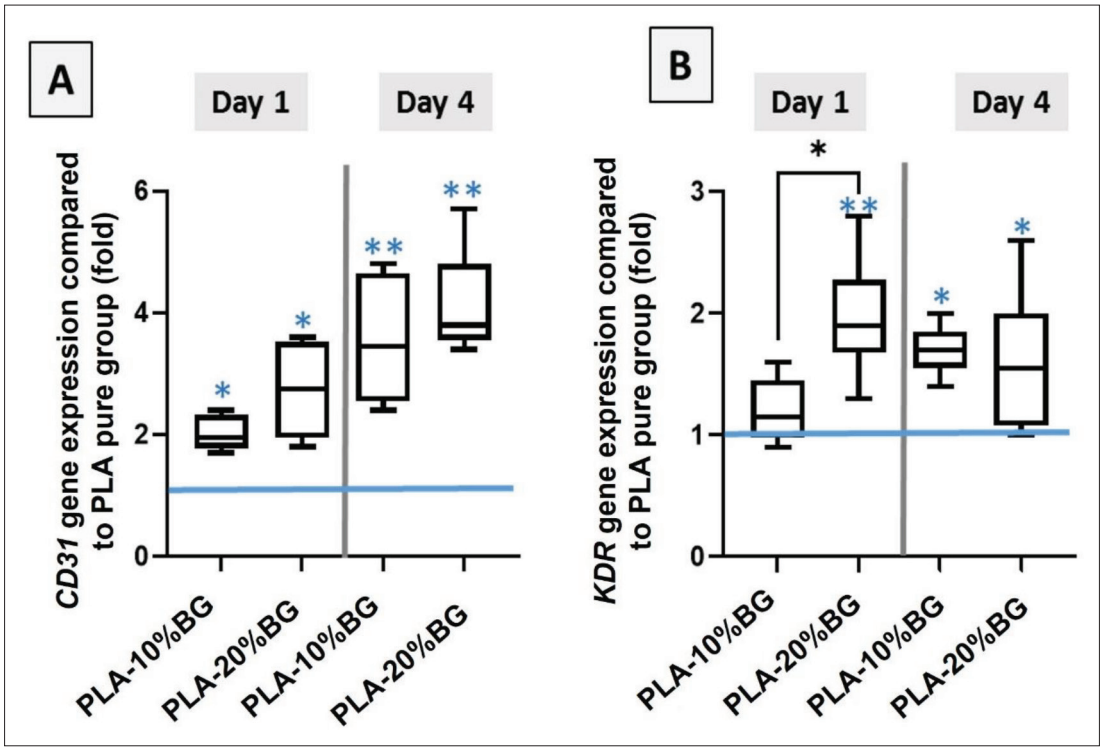

Figure 6. Gene expression analyses on PLA–10%BG and PLA–20%BG on day 1 and day 4 after seeding of HUVECs. Mann–Whitney *U* tests revealed significant differences (*$P < 0.05$, **$P < 0.01$, ***$P < 0.005$; ****$P < 0.001$). Black asterisk demonstrates significant difference between the PLA–10%BG and PLA–20%BG groups; light blue asterisk represents the significant difference compared to PLA pure group (blue line = 1). For a better overview, only the significant differences are indicated.

Only few studies have analyzed the effect of BG *in ovo*. Cohrs *et al.*[46] analyzed silicone elastomers blended with BG nano- (nBG) or micro-particles (mBG) *in ovo*. They found that nBG and mBG were better integrated into the membrane, but they displayed a lower vascular density. This group worked with a low BG concentration of 5%, a concentration with which we could not detect any positive effects on angiogenesis *in vitro*. Adipose tissue-derived stem cells seeded on a combination of polypropylene and BG demonstrated increased vascularization in the CAM assay, as measured by tube length[27]. Other groups used the CAM assay to show the biocompatibility or bone mineralization potential of BG-based scaffolds[47].

Besides the fact that the CAM assay demonstrates the positive effect on angiogenesis, this assay also confirms the biocompatibility of the PLA–BG material. The CAM assay is a well-accepted method to prove the biocompatibility of biomaterials and tissue-engineered constructs *in ovo* and *in vivo*[48,49]. It has been demonstrated that PLA and BG can be used as composite material and that the shape can be customized by 3D printing[50]. One advantage of 3D printing is the variation capacity—thickness, diameter, and pore size can be modified depending on the application. All these parameters can affect osteogenesis as well as angiogenesis as described before[25,51,52]. To analyze these parameters, the PLA–BG composite material will be applied in a follow-up *in vivo* study in a femur defect in the rat to further define the biocompatibility as well as the effect of different thicknesses and pore sizes in the scaffold. Another topic that will be analyzed in the animal model is the osteoimmunity regulating effects of the scaffold as it has been demonstrated that PLA/HA scaffolds induce osteoimmunity[53].

In the present study, we showed that the 3D-printed PLA–BG, especially at a BG concentration of 20%, induces angiogenesis *in vitro* with endothelial cells (HUVECs) as well as *in ovo*, as demonstrated in the CAM assay. PLA has been established as a degradable implant material in various biomedical areas like bone fixation, surgical implants, or scaffolds for bone tissue engineering[54]. However, there have been criticisms regarding the acidic pH following degradation of the scaffold[55], which has been disproven in a long-term study on horses[56]. By combining PLA with BG, the acidic degradation products are even further neutralized[55]. Another positive effect of the encapsulation of BG in PLA is the slower and continuous release of components. Other studies reported a very fast release rate causing cytotoxic effects[57].The released ions from BG are

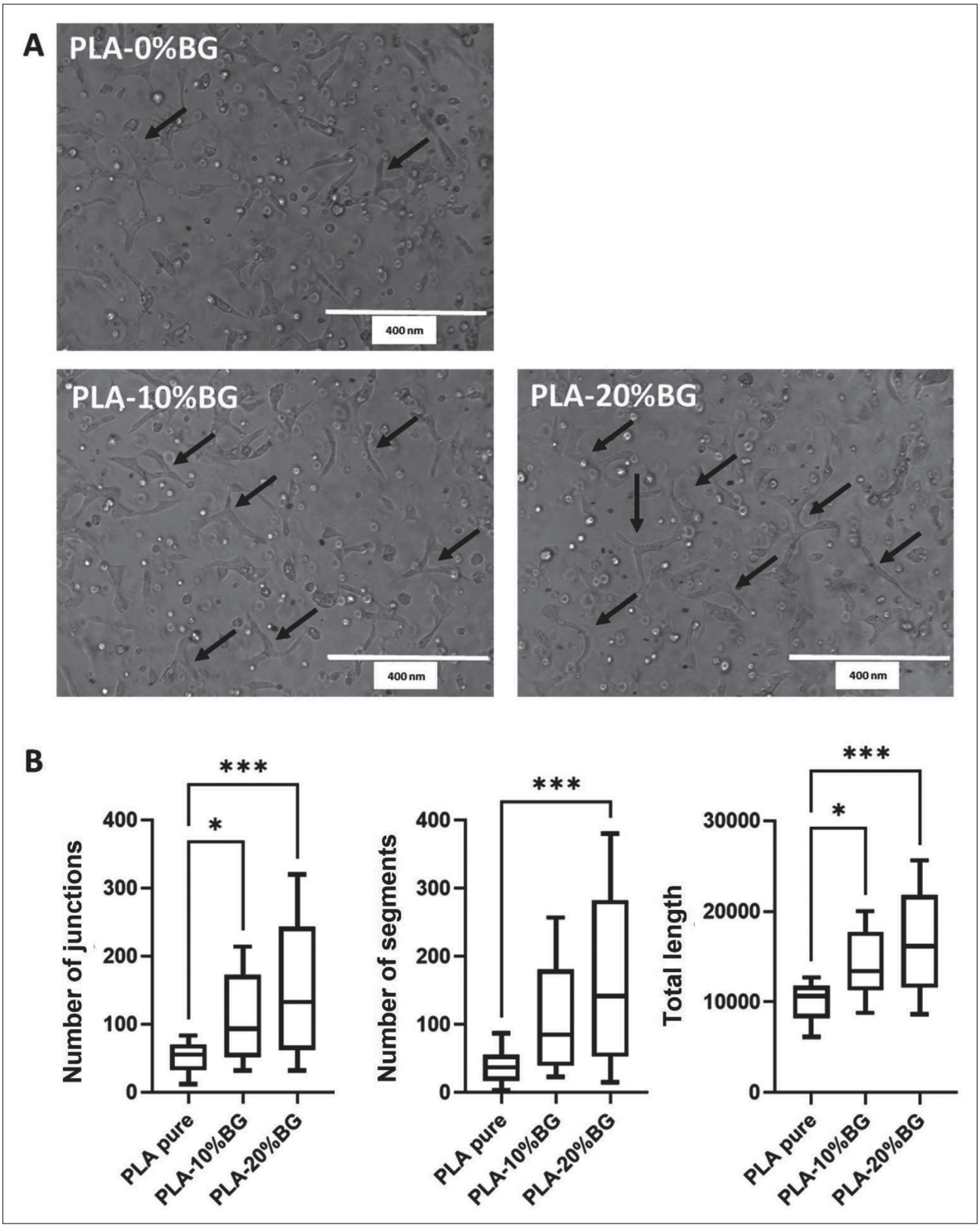

Figure 7. Matrigel assay with conditioned medium. (A) Exemplary illustrations of HUVECs in Matrigel® incubated with conditioned medium. Black arrows indicate segments and junctions. (B) Quantitative analyses as described in methods and Figure 1. All three analyzed components (number of junctions, number of segments and total length) increased with the BG concentration in the 3D-printed scaffolds. Mann–Whitney *U* tests revealed significant differences (*$P < 0.05$, **$P < 0.01$, ***$P < 0.005$; ****$P < 0.001$). For a better overview, only the significant differences are indicated.

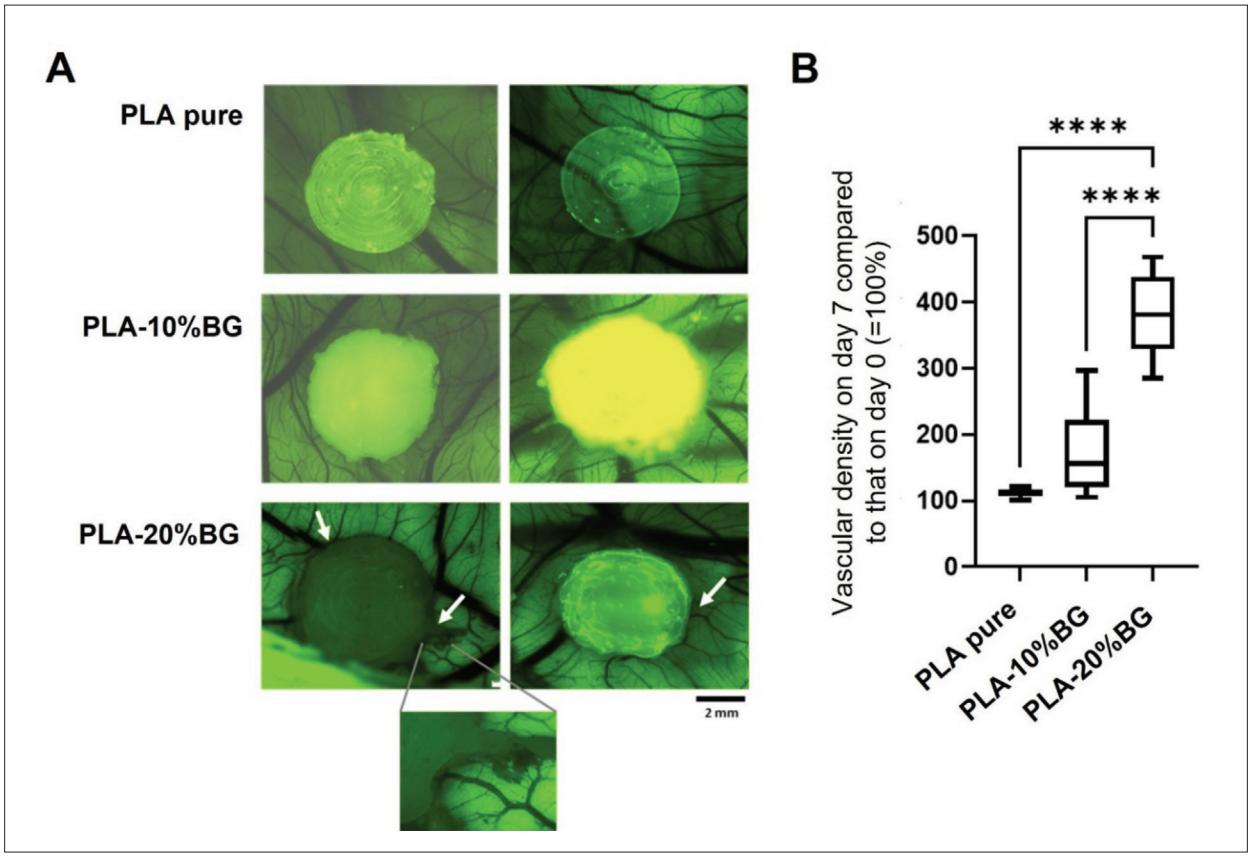

Figure 8. CAM assay. (A) Exemplary microscope images after 7 days of placement. (B) Quantification of vascular density. Mann-Whitney *U* tests revealed significant differences (*$p < 0.05$, **$p < 0.01$, ***$p < 0.005$; ****$p < 0.001$). For a better overview, only the significant differences are indicated.

Si, Ca, Na, and P[17,58], and it has been proposed that the release of these ions positively affects the osteogenesis as well as the angiogenic potential of human cells[47,58].

4. Conclusion and outlook

In this work, we demonstrated the angiogenic efficiency of a 3D-printed PLA–BG composite material, as an addition to our earlier work on the osteogenic potential of this material[16,17]. Taken together, we manufactured a mechanically stable, 3D-printable, osteogenic, and angiogenic material, which could be used for bone tissue engineering. *In vivo* analyses will be performed in future studies to confirm the *in vitro* results regarding biocompatibility and the osteogenic as well as angiogenic effects. Moreover, the degradability of the PLA–BG composite material will also be determined in the *in vivo* experiments.

In further work, we will also determine the antimicrobial activity of the 3D-printed composite material as it has been shown that BG inhibits the growth of various bacterial strains[59]. As infections are still a major problem in implant surgery, a material combining osteogenic, angiogenic, and antibacterial properties would solve many problems in this area.

Acknowledgments

We thank Simone Mendler, Department of Otorhinolaryngology, University Medical Center Mainz, for support with the CAM assays.

Funding

This research was funded by RMU-Initiativfond Forschung (Förderlinie 2).

Conflict of interest

The authors declare no conflict of interest.

Author contributions

Conceptualization: Ulrike Ritz, Dirk Henrich, Eva Schätzlein, Andreas Blaeser, Johannes Frank

Data curation: Simon Cichos

Formal analysis: Ulrike Ritz, Nadine Wiesmann-Imilowski

Funding acquisition: Ulrike Ritz, Dirk Henrich, Andreas Blaeser, Johannes Frank, Philipp Drees, Erol Gercek
Investigation: Simon Cichos, Nadine Wiesmann-Imilowski
Methodology: Simon Cichos, Eva Schätzlein, Nadine Wiesmann-Imilowski
Project administration: Ulrike Ritz, Dirk Henrich, Andreas Blaeser
Resources: Eva Schätzlein, Ulrike Ritz, Dirk Henrich, Andreas Blaeser, Philipp Drees, Erol Gercek
Supervision: Ulrike Ritz, Dirk Henrich Andreas Blaeser
Validation: Ulrike Ritz
Visualization: Ulrike Ritz, Eva Schätzlein, Johannes Frank, Dirk Henrich
Writing – original draft: Ulrike Ritz, Simon Cichos
Writing – review & editing: Eva Schätzlein, Nadine Wiesmann-Imilowski, Andreas Blaeser, Dirk Henrich, Johannes Frank, Philipp Drees, Erol Gercek

All authors have read and agreed to the published version of the manuscript.

Ethics approval and consent to participate

Not applicable.

Consent for publication

Not applicable.

Availability of data

The data that support the findings of this study are available on request from the corresponding author.

References

1. Karalashvili L, Kakabadze A, Uhryn M, *et al.*, 2018, Bone grafts for reconstruction of bone defects (review). *Georgian Med News*, 282:44–49.

2. Schmidt AH, 2021, Autologous bone graft: Is it still the gold standard? *Injury*, 52(Suppl 2):S18–S22.

   https://doi.org/10.1016/j.injury.2021.01.043

3. Arif ZU, Khalid MY, Noroozi R, *et al.*, 2022, Recent advances in 3D-printed polylactide and polycaprolactone-based biomaterials for tissue engineering applications. *Int J Biol Macromol*, 218:930–968.

   https://doi.org/10.1016/j.ijbiomac.2022.07.140

4. Kaya I, Sahin MC, Cingoz ID, *et al.*, 2019, Three dimensional printing and biomaterials in the repairment of bone defects; hydroxyapatite PLA filaments. *Turk J Med Sci*, 49(3):922–927.

   https://doi.org/10.3906/sag-1901-184

5. Liu T, Li B, Chen G, *et al.*, 2022, Nano tantalum-coated 3D printed porous polylactic acid/beta-tricalcium phosphate scaffolds with enhanced biological properties for guided bone regeneration. *Int J Biol Macromol*, 221:371–380.

   https://doi.org/10.1016/j.ijbiomac.2022.09.003

6. Alksne M, Kalvaityte M, Simoliunas E, *et al.*, 2020, In vitro comparison of 3D printed polylactic acid/hydroxyapatite and polylactic acid/bioglass composite scaffolds: Insights into materials for bone regeneration. *J Mech Behav Biomed Mater*, 104:103641.

   https://doi.org/10.1016/j.jmbbm.2020.103641

7. Hench LL, Jones JR, 2015, Bioactive glasses: Frontiers and challenges. *Front Bioeng Biotechnol*, 3:194.

   https://doi.org/10.3389/fbioe.2015.00194

8. Zare S, Mohammadpour M, Izadi Z, *et al.*, 2022, Nanofibrous hydrogel nanocomposite based on strontium-doped bioglass nanofibers for bone tissue engineering applications. *Biology (Basel)*, 11(10).

   https://doi.org/10.3390/biology11101472

9. Kumari S, Singh D, Srivastava P, *et al.*, 2022, Generation of graphene oxide and nano-bioglass based scaffold for bone tissue regeneration. *Biomed Mater*, 17(6).

   https://doi.org/10.1088/1748-605X/ac92b4

10. Kukulka EC, de Souza JR, de Araujo JCR, *et al.*, 2023, Polycaprolactone/chlorinated bioglass scaffolds doped with Mg and Li ions: Morphological, physicochemical, and biological analysis. *J Biomed Mater Res B Appl Biomater*, 111(1):140–150.

    https://doi.org/10.1002/jbm.b.35140

11. Daskalakis E, Huang B, Vyas C, *et al.*, 2022, Novel 3D bioglass scaffolds for bone tissue regeneration. *Polymers (Basel)*, 14(3).

    https://doi.org/10.3390/polym14030445

12. Blaker JJ, Gough JE, Maquet V, *et al.*, 2003, In vitro evaluation of novel bioactive composites based on bioglass-filled polylactide foams for bone tissue engineering scaffolds. *J Biomed Mater Res A*, 67(4):1401–1411.

    https://doi.org/10.1002/jbm.a.20055

13. Maquet V, Boccaccini AR, Pravata L, *et al.*, 2003, Preparation, characterization, and in vitro degradation of bioresorbable and bioactive composites based on bioglass-filled polylactide foams. *J Biomed Mater Res A*, 66(2):335–346.

    https://doi.org/10.1002/jbm.a.10587

14. Roether JA, Boccaccini AR, Hench LL, *et al.*, 2002, Development and in vitro characterisation of novel bioresorbable and bioactive composite materials based on polylactide foams and bioglass for tissue engineering applications. *Biomaterials*, 23(18):3871–3878.

    https://doi.org/10.1016/s0142-9612(02)00131-x

15. Lyyra I, Leino K, Hukka T, *et al.*, 2021, Impact of glass composition on hydrolytic degradation of polylactide/bioactive glass composites. *Materials (Basel)*, 14(3).

    https://doi.org/10.3390/ma14030667

16. Söhling N, Neijhoft J, Nienhaus V, *et al.*, 2020, 3D-printing of hierarchically designed and osteoconductive bone tissue engineering scaffolds. *Materials (Basel)*, 13(8).

    https://doi.org/10.3390/ma13081836

17. Schätzlein E, Kicker C, Söhling N, *et al.*, 2022, 3D-printed PLA-bioglass scaffolds with controllable calcium release and MSC adhesion for bone tissue engineering. *Polymers (Basel)*, 14(12).

    https://doi.org/10.3390/polym14122389

18. Söhling N, Al Zoghool S, Schätzlein E, *et al.*, 2022, In vitro evaluation of a 20% bioglass-containing 3D printable PLA composite for bone tissue engineering. *Int J Bioprint*, 8(4):602.

    https://doi.org/10.18063/ijb.v8i4.602

19. Giannoudis PV, Atkins R, 2007, Management of long-bone non-unions. *Injury*, 38(Suppl 2):S1–S2.

20. Andrzejowski P, Giannoudis PV, 2019, The 'diamond concept' for long bone non-union management. *J Orthop Traumatol*, 20(1):21.

    https://doi.org/10.1186/s10195-019-0528-0

21. Mahapatra C, Kumar P, Paul MK, *et al.*, 2022, Angiogenic stimulation strategies in bone tissue regeneration. *Tissue Cell*, 79:101908.

    https://doi.org/10.1016/j.tice.2022.101908

22. Rather HA, Jhala D, Vasita R, 2019, Dual functional approaches for osteogenesis coupled angiogenesis in bone tissue engineering. *Mater Sci Eng C Mater Biol Appl*, 103:109761.

    https://doi.org/10.1016/j.msec.2019.109761

23. Tsiridis E, Upadhyay N, Giannoudis P, 2007, Molecular aspects of fracture healing: Which are the important molecules? *Injury*, 38(Suppl 1):S11–S25.

    https://doi.org/10.1016/j.injury.2007.02.006

24. Zhao D, Zhu T, Li J, *et al.*, 2021, Poly(lactic-co-glycolic acid)-based composite bone-substitute materials. *Bioact Mater,* 6(2):346–360.

    https://doi.org/10.1016/j.bioactmat.2020.08.016

25. Zhu T, Jiang M, Zhang M, *et al.*, 2022, Biofunctionalized composite scaffold to potentiate osteoconduction, angiogenesis, and favorable metabolic microenvironment for osteonecrosis therapy. *Bioact Mater*, 9:446–460.

    https://doi.org/10.1016/j.bioactmat.2021.08.005

26. Li H, He J, Yu H, *et al.*, 2016, Bioglass promotes wound healing by affecting gap junction connexin 43 mediated endothelial cell behavior. *Biomaterials*, 84:64–75.

    https://doi.org/10.1016/j.biomaterials.2016.01.033

27. Handel M, Hammer TR, Nooeaid P, *et al.*, 2013, 45S5-bioglass((R))-based 3D-scaffolds seeded with human adipose tissue-derived stem cells induce in vivo vascularization in the CAM angiogenesis assay. *Tissue Eng Part A*, 19(23–24):2703–2712.

    https://doi.org/10.1089/ten.TEA.2012.0707

28. Deb S, Mandegaran R, Di Silvio L, 2010, A porous scaffold for bone tissue engineering/45S5 bioglass derived porous scaffolds for co-culturing osteoblasts and endothelial cells. *J Mater Sci Mater Med*, 21(3):893–905.

    https://doi.org/10.1007/s10856-009-3936-5

29. Stähli C, James-Bhasin M, Hoppe A, *et al.*, 2015, Effect of ion release from Cu-doped 45S5 bioglass(R) on 3D endothelial cell morphogenesis. *Acta Biomater*, 19:15–22.

    https://doi.org/10.1016/j.actbio.2015.03.009

30. Eldesoqi K, Seebach C, Nguyen Ngoc C, *et al.*, 2013, High calcium bioglass enhances differentiation and survival of endothelial progenitor cells, inducing early vascularization in critical size bone defects. *PLoS One*, 8(11):e79058.

    https://doi.org/10.1371/journal.pone.0079058

31. Barbeck M, Serra T, Booms P, *et al.*, 2017, Analysis of the in vitro degradation and the in vivo tissue response to bi-layered 3D-printed scaffolds combining PLA and biphasic PLA/bioglass components—Guidance of the inflammatory response as basis for osteochondral regeneration. *Bioact Mater*, 2(4):208–223.

    https://doi.org/10.1016/j.bioactmat.2017.06.001

32. Livak KJ, Schmittgen TD, 2001, Analysis of relative gene expression data using real-time quantitative PCR and the 2(-Delta Delta C(T)) method. *Methods,* 25(4):402–408.

    https://doi.org/10.1006/meth.2001.1262

33. Carpentier G, Berndt S, Ferratge S, *et al.*, 2020, Angiogenesis analyzer for ImageJ—A comparative morphometric analysis of "Endothelial Tube Formation Assay" and "Fibrin Bead Assay". *Sci Rep*, 10(1):11568.

    https://doi.org/10.1038/s41598-020-67289-8

34. Buhr CR, Wiesmann N, Tanner RC, *et al.*, 2020, The chorioallantoic membrane assay in nanotoxicological research—An alternative for in vivo experimentation. *Nanomaterials (Basel)*, 10(12).

    https://doi.org/10.3390/nano10122328

35. Ribatti D, Annese T, Tamma R, 2020, The use of the chick embryo CAM assay in the study of angiogenic activiy of biomaterials. *Microvasc Res*, 131:104026.

    https://doi.org/10.1016/j.mvr.2020.104026

36. Yu Y, Yang B, Tian D, *et al.*, 2022, Thiolated hyaluronic acid/silk fibroin dual-network hydrogel incorporated with bioglass nanoparticles for wound healing. *Carbohydr Polym*, 288:119334.

    https://doi.org/10.1016/j.carbpol.2022.119334

37. Wu Z, He D, Li H, 2021, Bioglass enhances the production of exosomes and improves their capability of promoting vascularization. *Bioact Mater*, 6(3):823–835.

https://doi.org/10.1016/j.bioactmat.2020.09.011

38. El-Gendy R, Kirkham J, Newby PJ, *et al.*, 2015, Investigating the vascularization of tissue-engineered bone constructs using dental pulp cells and 45S5 bioglass(R) scaffolds. *Tissue Eng Part A*, 21(13–14):2034–2043.

https://doi.org/10.1089/ten.tea.2014.0485

39. El-Gendy R, Yang XB, Newby PJ, *et al.*, 2013, Osteogenic differentiation of human dental pulp stromal cells on 45S5 bioglass(R) based scaffolds in vitro and in vivo. *Tissue Eng Part A*, 19(5–6):707–715.

https://doi.org/10.1089/ten.TEA.2012.0112

40. Ponce ML, 2009, Tube formation: An in vitro Matrigel angiogenesis assay. *Methods Mol Biol*, 467:183–188.

https://doi.org/10.1007/978-1-59745-241-0_10

41. Benton G, Arnaoutova I, George J, *et al.*, 2014, Matrigel: From discovery and ECM mimicry to assays and models for cancer research. *Adv Drug Deliv Rev*, 79-80:3–18.

https://doi.org/10.1016/j.addr.2014.06.005

42. Fischer D, Fluegen G, Garcia P, *et al.*, 2022, The CAM model-Q&A with experts. *Cancers (Basel)*, 15(1).

https://doi.org/10.3390/cancers15010191

43. Weber J, Weber M, Steinle H, *et al.*, 2021, An alternative in vivo model to evaluate pluripotency of patient-specific iPSCs. *ALTEX*, 38(3):442–450.

https://doi.org/10.14573/altex.2005221

44. Ribatti D, 2014, The chick embryo chorioallantoic membrane as a model for tumor biology. *Exp Cell Res*, 328(2):314–324.

https://doi.org/10.1016/j.yexcr.2014.06.010

45. Hagedorn M, Balke M, Schmidt A, *et al.*, 2004, VEGF coordinates interaction of pericytes and endothelial cells during vasculogenesis and experimental angiogenesis. *Dev Dyn*, 230(1):23–33.

https://doi.org/10.1002/dvdy.20020

46. Cohrs NH, Schulz-Schonhagen K, Mohn D, *et al.*, 2019, Modification of silicone elastomers with bioglass 45S5(R) increases in ovo tissue biointegration. *J Biomed Mater Res B Appl Biomater*, 107(4):1180–1188.

https://doi.org/10.1002/jbm.b.34211

47. Vargas GE, Mesones RV, Bretcanu O, *et al.*, 2009, Biocompatibility and bone mineralization potential of 45S5 bioglass-derived glass-ceramic scaffolds in chick embryos. *Acta Biomater*, 5(1):374–380.

https://doi.org/10.1016/j.actbio.2008.07.016

48. Mangir N, Dikici S, Claeyssens F, *et al.*, 2019, Using ex ovo chick chorioallantoic membrane (CAM) assay to evaluate the biocompatibility and angiogenic response to biomaterials. *ACS Biomater Sci Eng*, 5(7):3190–3200.

https://doi.org/10.1021/acsbiomaterials.9b00172

49. Baiguera S, Macchiarini P, Ribatti D, 2012, Chorioallantoic membrane for in vivo investigation of tissue-engineered construct biocompatibility. *J Biomed Mater Res B Appl Biomater*, 100(5):1425–1434.

https://doi.org/10.1002/jbm.b.32653

50. Brezulier D, Chaigneau L, Jeanne S, *et al.*, 2021, The challenge of 3D bioprinting of composite natural polymers PLA/bioglass: Trends and benefits in cleft palate surgery. *Biomedicines*, 9(11).

https://doi.org/10.3390/biomedicines9111553

51. Kasten P, Beyen I, Niemeyer P, *et al.*, 2008, Porosity and pore size of beta-tricalcium phosphate scaffold can influence protein production and osteogenic differentiation of human mesenchymal stem cells: An in vitro and in vivo study. *Acta Biomater*, 4(6):1904–1915.

https://doi.org/10.1016/j.actbio.2008.05.017

52. Hoemann CD, Rodriguez Gonzalez J, Guzman-Morales J, *et al.*, 2022, Chitosan coatings with distinct innate immune bioactivities differentially stimulate angiogenesis, osteogenesis and chondrogenesis in poly-caprolactone scaffolds with controlled interconnecting pore size. *Bioact Mater*, 10:430–442.

https://doi.org/10.1016/j.bioactmat.2021.09.012

53. Zhang J, Tong D, Song H, *et al.*, 2022, Osteoimmunity-regulating biomimetically hierarchical scaffold for augmented bone regeneration. *Adv Mater*, 34(36):e2202044.

https://doi.org/10.1002/adma.202202044

54. Finotti PF, Costa LC, Capote TS, *et al.*, 2017, Immiscible poly(lactic acid)/poly(epsilon-caprolactone) for temporary implants: Compatibility and cytotoxicity. *J Mech Behav Biomed Mater*, 68:155–162.

https://doi.org/10.1016/j.jmbbm.2017.01.050

55. Diomede F, Gugliandolo A, Cardelli P, *et al.*, 2018, Three-dimensional printed PLA scaffold and human gingival stem cell-derived extracellular vesicles: A new tool for bone defect repair. *Stem Cell Res Ther*, 9(1):104.

https://doi.org/10.1186/s13287-018-0850-0

56. Carvalho JRG, Conde G, Antonioli ML, *et al.*, 2021, Long-term evaluation of poly(lactic acid) (PLA) implants in a horse: An experimental pilot study. *Molecules,* 26(23).

https://doi.org/10.3390/molecules26237224

57. Fernandes HR, Gaddam A, Rebelo A, *et al.*, 2018, Bioactive glasses and glass-ceramics for healthcare applications in bone regeneration and tissue engineering. *Materials (Basel)*, 11(12).

https://doi.org/10.3390/ma11122530

58. Hoppe A, Guldal NS, Boccaccini AR, 2011, A review of the biological response to ionic dissolution products from bioactive glasses and glass-ceramics. *Biomaterials*, 32(11):2757–2774.

https://doi.org/10.1016/j.biomaterials.2011.01.004

59. Zhou P, Garcia BL, Kotsakis GA, 2022, Comparison of antibacterial and antibiofilm activity of bioactive glass compounds S53P4 and 45S5. *BMC Microbiol*, 22(1):212.

https://doi.org/10.1186/s12866-022-02617-8